

Impaired Cholesterol Efflux in Senescent Macrophages Promotes Age-Related Macular Degeneration

Abdoulaye Sene,^{1,8} Aslam A. Khan,^{1,8} Douglas Cox,¹ Rei E.I. Nakamura,¹ Andrea Santeford,¹ Bryan M. Kim,¹ Rohini Sidhu,² Michael D. Onken,¹ J. William Harbour,¹ Shira Hagbi-Levi,⁴ Itay Chowers,⁴ Peter A. Edwards,⁵ Angel Baldan,⁶ John S. Parks,⁷ Daniel S. Ory,² and Rajendra S. Apte^{1,3,*}

¹Department of Ophthalmology and Visual Sciences

²Diabetic Cardiovascular Disease Center

³Department of Developmental Biology

Washington University School of Medicine, Saint Louis, MO 63110, USA

⁴Hadassah-Hebrew University Medical Center, Jerusalem 91120, Israel

⁵Department of Biological Chemistry, David Geffen School of Medicine, University of California, Los Angeles, Los Angeles, CA 90095, USA

⁶Edward A. Doisy Department of Biochemistry and Molecular Biology, Saint Louis University, Saint Louis, MO 63104, USA

⁷Department of Pathology/Section on Lipid Sciences and Department of Biochemistry, Wake Forest School of Medicine, Winston-Salem, NC 27157, USA

⁸These authors contributed equally to this work

*Correspondence: apte@vision.wustl.edu

<http://dx.doi.org/10.1016/j.cmet.2013.03.009>

SUMMARY

Pathologic angiogenesis mediated by abnormally polarized macrophages plays a central role in common age-associated diseases such as atherosclerosis, cancer, and macular degeneration. Here we demonstrate that abnormal polarization in older macrophages is caused by programmatic changes that lead to reduced expression of ATP binding cassette transporter ABCA1. Downregulation of ABCA1 by microRNA-33 impairs the ability of macrophages to effectively efflux intracellular cholesterol, which in turn leads to higher levels of free cholesterol within senescent macrophages. Elevated intracellular lipid polarizes older macrophages to an abnormal, alternatively activated phenotype that promotes pathologic vascular proliferation. Mice deficient for *Abca1*, but not *Abcg1*, demonstrate an accelerated aging phenotype, whereas restoration of cholesterol efflux using LXR agonists or miR-33 inhibitors reverses it. Monocytes from older humans with age-related macular degeneration showed similar changes. These findings provide an avenue for therapeutic modulation of macrophage function in common age-related diseases.

INTRODUCTION

Macrophage-mediated inflammation is causative in several age-associated diseases, including atherosclerotic heart disease, cancers, and blinding eye diseases such as age-related macular degeneration (AMD) (Apte et al., 2006; Kelly et al., 2007; Moore and Tabas, 2011; Nakao et al., 2005; Niederkorn, 2006). In atherosclerotic plaques, cholesterol-loaded foam cell macro-

phages can incite inflammatory rupture of plaques and can lead to life-threatening cardiovascular complications (Moore and Tabas, 2011; Tall et al., 2008). In the aged eye, alternatively activated macrophages can promote pathologic angiogenesis underneath the retina that leads to blindness (Apte et al., 2006; Kelly et al., 2007).

ABCA1 and ABCG1 are members of the ATP binding cassette (ABC) family of transporters and play critical roles in mobilizing cholesterol out of macrophages and onto extracellular high-density lipoprotein (HDL). ABCA1 promotes binding of apolipoprotein A-1 (ApoA-1) to the cell surface, where it solubilizes membrane phospholipid and cholesterol to form nascent HDL particles in the extracellular space (Vedhachalam et al., 2007). Unlike ABCA1, ABCG1 cellular localization and its involvement in cholesterol transport are controversial. Although ABCG1 has been identified as a key player in macrophage cholesterol transport, studies with genetically modified mice revealed that ABCG1 accounted for little of the cellular cholesterol efflux and subsequent plasma lipoprotein levels (Kennedy et al., 2005; Nakamura et al., 2004; Tarling and Edwards, 2011b). Recent studies reported that ABCG1 was mainly mobilized to intracellular vesicles of the endosomal pathway to transfer sterols to the plasma membrane, in contrast to the previous reports of localization of ABCG1 to the cell membrane (Tarling and Edwards, 2011a).

ABCA1 and ABCG1 may act sequentially, with ABCA1 generating nascent HDL particles and ABCG1 promoting additional cholesterol efflux onto HDL, LDL, liposomes, or cyclodextrin, in a nonspecific manner. In macrophage-specific *Abca1*^{-M/-M} mice, there is accumulation of free cholesterol within these cells, increased lipid rafts content in the plasma membrane, increased Toll-like receptor 4 in lipid rafts, and increased proinflammatory activation of macrophages in response to Toll-like receptor agonists (Zhu et al., 2008).

AMD is the leading cause of blindness in elderly individuals over 50 years of age in the industrialized world. Blindness in AMD occurs largely from the exudative (wet) form of the disease that is characterized by the development of abnormal blood

vessels underneath the retina, also called choroidal neovascularization (CNV) (see [Figure S1A](#) online) ([Klein et al., 2004](#); [van Leeuwen et al., 2003](#)). Senescent macrophages have been shown to polarize to a proangiogenic phenotype and promote the development of CNV ([Kelly et al., 2007](#)). Wet AMD is preceded by nonexudative (dry) AMD. Dry or early AMD is diagnosed by the presence of lipid-rich deposits called drusen that develop external to the retinal pigment epithelium (RPE) underneath the retina ([Figure S1B](#)). Drusen are cardinal features of dry AMD ([Hageman et al., 2001](#)). Drusen have high lipid content characterized by esterified-cholesterol-rich apolipoprotein-B-containing lipoproteins (ApoB-LPs). ApoB-LPs accumulate within drusen, as has been reported in atherosclerotic plaques ([Curcio et al., 2001, 2005, 2009, 2010](#); [Wang et al., 2010](#)). These deposits can serve as a nidus for monocytic inflammation ([Curcio et al., 2009](#)). Progression of AMD is often characterized by increased size and number of these lipid-rich drusen ([Bressler et al., 1990](#)). Macrophages have been shown to extend dendritic processes into drusen, and macrophage-mediated inflammation accelerates the conversion of dry to wet form of AMD by promoting blinding pathogenic neovascularization underneath drusen ([Apte et al., 2006](#); [Kelly et al., 2007](#)). Specifically, programmatic changes in macrophage activation associated with senescence polarize these cells to a proangiogenic or alternatively activated phenotype characterized by increased expression of IL-10 and decreased expression of IL-6 and TNF- α , among others. These alternatively activated macrophages promote the development of CNV that leads to progressive loss of vision. The precise mechanisms by which “old” macrophages polarize to a proangiogenic phenotype are yet unknown.

There has been recent interest in the association of cholesterol regulatory pathways and advanced AMD. Genome-wide association studies (GWAS) have demonstrated that single nucleotide polymorphisms (SNPs) in the innate immune system, specifically in the complement regulatory pathway, increase the risk of development and progression of AMD ([Edwards et al., 2005](#)). GWAS have also demonstrated an association between SNPs in genes involved in cholesterol metabolism and advanced AMD. These include *Abca1*, cholesteryl ester transfer protein (*CETP*), hepatic triglyceride lipase C (*LIPC*), and lipoprotein lipase (*LPL*) ([Chen et al., 2010](#); [Neale et al., 2010](#)). These polymorphisms are especially interesting because multivariate analyses have shown that allelic associations with advanced AMD are independent of actual serum HDL or lipid levels. It is thus apparent that the biologic pathways that connect macrophage-mediated inflammation, cholesterol regulation, and age in eye disease and drusen are highly complex and cannot be explained by a simple association between increased risk and abnormal serum lipid component levels. We investigated the potential link between abnormal lipid regulation in the senescent macrophage and its effects on inflammation-driven angiogenesis in age-associated eye disease.

RESULTS

Aging-Impaired Macrophage Cholesterol Efflux Capacity

To determine whether age altered cholesterol efflux in macrophages, we analyzed the expression patterns of ABCA1 and

ABCG1 in these cells. Quantitative analysis of gene expression by real-time PCR demonstrated an age-associated reduction in levels of ABCA1 and ABCG1 expression in splenic, peritoneal, and eye macrophages and PBMCs ([Figures 1A–1D](#) and [Figure S1C](#)). Analysis of ABCA1 and ABCG1 protein levels in peritoneal macrophages isolated from either young (<3 months) or old (>18 months) mice by western blotting, and flow cytometry confirmed that reduced gene expression of ABCA1 and ABCG1 with age translated to reduced protein expression ([Figures 1E](#) and [1F](#)).

Because of the critical role of ABC transporters in lipid metabolism in macrophages, we examined whether the age-associated decrease of ABCA1 and ABCG1 altered the intracellular lipid load within macrophages and influenced formation of foam cells. Thioglycollate-elicited young or old peritoneal macrophages were stained with oil red O to visualize foam cells ([Figure 2A](#), arrow). Quantitative analysis of lipid-laden macrophages showed that foamy macrophages were more frequent in peritoneal macrophages collected from old mice as compared to young mice ([Figure 2B](#)). Subsequent quantification of total cholesterol content by fluorometry confirmed the significantly increased accumulation of cholesterol in old macrophages compared to their young counterparts (21.95 ± 0.15 versus 14.90 ± 0.10 , $p < 0.001$) ([Figure 2C](#)). To test whether the senescence-associated decrease of ABC transporters affected the cholesterol efflux efficiency in macrophages, we assessed the ability of peritoneal macrophages to effectively internalize, retain, and subsequently efflux lipids from oxidized low-density lipoproteins (oxLDL). Thioglycollate-elicited young or old peritoneal macrophages were incubated with Dil-oxLDL for 24 hr, following which cells were washed and incubated in fresh media. Intracellular accumulation of Dil-oxLDL was then examined by confocal microscopy. Macrophages from old mice had higher levels of intracellular oxLDL compared to macrophages from young mice ([Figure 2D](#)). In order to assess their abilities to efflux lipids, young and old macrophages were incubated with Dil-oxLDL for 3 hr, following which cells were washed and incubated in fresh media for an additional 21 hr. There was no difference in the level of internalized oxLDL in young as compared to old macrophage examined by fluorescence microscopy immediately after 3 hr of incubation, confirming that the influx capacity of old macrophages was not altered (data not shown). However, quantitative analysis of the extruded oxLDL content showed significantly higher levels in supernatants of young macrophages compared to old cells ([Figure S2](#)).

As Dil-oxLDL is not a direct and specific measure of cholesterol efflux, we next analyzed specific cholesterol efflux of young and old macrophages preloaded with [^3H] cholesterol using ApoA1 and HDL as carriers. Macrophages were incubated with 5 $\mu\text{Ci/ml}$ [^3H]cholesterol-labeled oxLDL for 24 hr. Cells were washed and equilibrated for 1 hr followed by incubation for 4 hr in media containing ApoA1 or HDL. Consistent with the results above, we demonstrate that cholesterol efflux is significantly reduced in old macrophages ([Figure 2E](#)). Taken together, our findings demonstrate that reduced expression of ABC transporters in old macrophages impairs their ability to effectively efflux cholesterol.

It has been previously demonstrated that macrophages can sense alterations in extracellular cholesterol levels and

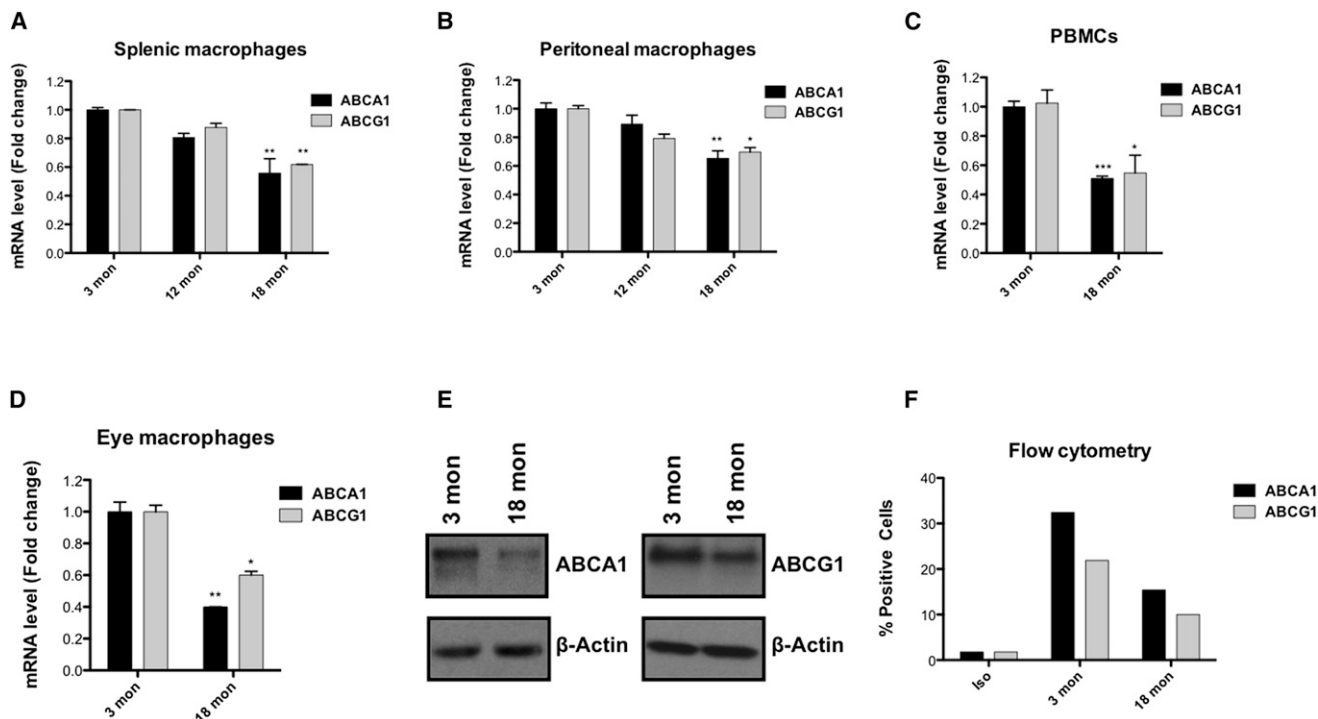


Figure 1. ABCA1 and ABCG1 Expression Is Altered in Senescent Macrophages

(A–C) Quantitative mRNA analysis of ABCA1 and ABCG1 in splenic (A) and peritoneal (B) macrophages and PBMCs (C) isolated from 3-, 12-, or 18-month-old mice.

(D) CNV was induced in 3- or 18-month-old mice, and eye macrophages harvested by laser microdissection were analyzed for ABCA1 and ABCG1 expression by qPCR.

(E) Whole-cell lysates of peritoneal macrophages of 3- or 18-month-old mice were subjected to immunoblot analysis with antibodies against ABCA1, ABCG1, or β -actin.

(F) Relative flow cytometry profiles of ABCA1 and ABCG1 in peritoneal macrophages isolated from 3- or 18-month-old mice. Iso, negative isotype control.

Values are expressed as mean + SE (A–D). Statistically significant difference, * $p < 0.05$, ** $p < 0.01$, *** $p < 0.001$.

effectively modulate levels of ABC transporters (Repa et al., 2000). We next investigated the effect of cholesterol treatment on the expression patterns of ABCA1/G1 in young or old macrophages. Young macrophages demonstrated a robust increase in expression of both ABCA1 and G1 after incubation with oxLDL, while old macrophages were significantly impaired in their ability to do so (Figures 2F and 2G). These findings confirm that senescent macrophages not only have reduced cholesterol efflux capacities but also are unable to respond to exogenous lipid as efficiently as young macrophages.

In response to microenvironmental signals, macrophages have been shown to exhibit classic (M1) or alternative (M2) activation characterized by differential cytokine production, receptor expression, and effector function (Mantovani et al., 2004; Mosser, 2003). We examined whether defective cholesterol efflux promoted a specific macrophage activation phenotype. In young and old macrophages, the gene expression profile of M1 (TNF- α , IL-6, IL1 β , PTGS2, CCL2, and MMP9) and M2 (IL-10, CD163, and TGF- β) markers was assessed by real-time PCR. As shown in Figure 2H, expression of M1 markers was significantly reduced in old as compared to young macrophages, whereas expression of M2 markers IL-10 and CD163 was significantly upregulated. These results clearly indicate that senescent

macrophages are alternatively activated and associated with an anti-inflammatory profile.

***Abca1*, Not *Abcg1*, Deletion Affected Macrophage Regulation of Vascular Endothelial Cell Proliferation and Pathological Angiogenesis**

To determine the contribution of individual ABC transporters in age-associated dysfunction of macrophage cholesterol homeostasis, we investigated the effects of selective *Abca1* or *Abcg1* deletion on effector function. Recent studies have demonstrated that macrophage polarization can play a pivotal role in determining their ultimate effector functions, including their ability to regulate angiogenesis (Apte et al., 2006; Kelly et al., 2007; Mantovani et al., 2005; Mosser, 2003). To determine whether *Abca1* or *Abcg1* deletion affected macrophage polarization, we analyzed the gene expression patterns of peritoneal macrophages isolated from young wild-type (WT), *Abca1*^{M/M}, or *Abcg1*^{−/−} mice by quantitative real-time PCR. Loss of *Abca1* was associated with a significant decrease in IL-6, IL1 β , PTGS2, and MMP9 expression and an upregulation of IL-10 expression, consistent with an alternatively activated phenotype (Figure 3A). Expression levels of TNF- α and IL-12 were not altered (data not shown). As previously shown, this gene

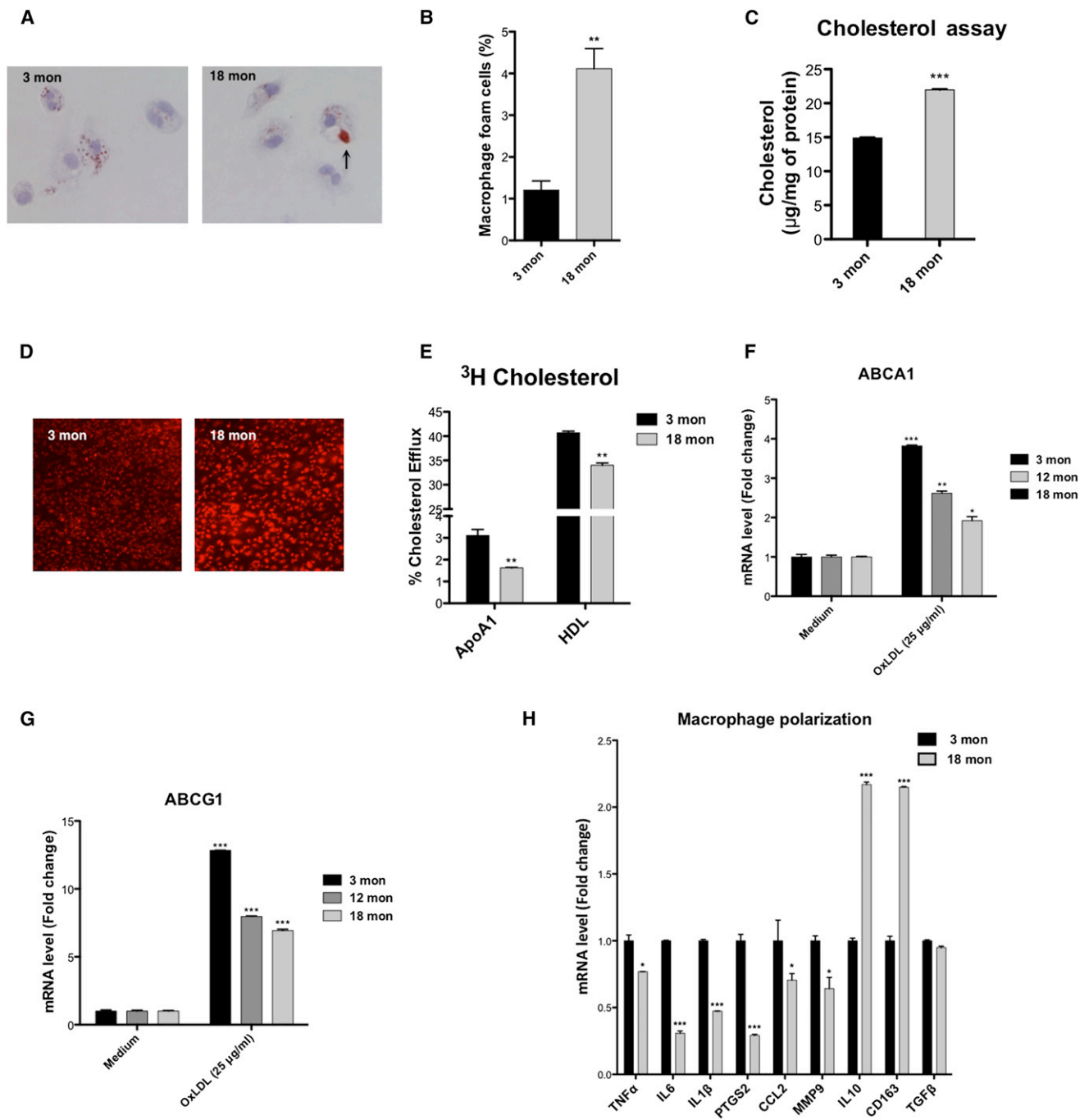


Figure 2. Age-Associated Impairment in Macrophage Cholesterol Efflux Capacities

(A and B) (A) Thioglycollate-elicited young or old peritoneal macrophages were stained with oil red O and hematoxylin, and (B) quantitative analysis of foamy macrophages was performed.

(C) Total cholesterol content of young or old macrophage was measured and normalized to protein content.

(D) Peritoneal macrophages were incubated with Dil-oxLDL, and intracellular accumulation of oxLDL was assessed by confocal microscopy.

(E) Cholesterol efflux to ApoA1 and HDL of peritoneal macrophages preloaded with [3 H]cholesterol-oxLDL.

(F and G) Peritoneal macrophages isolated from 3-, 12-, or 18-month-old mice were treated with 25 mg/ml oxLDL, and relative mRNA expression of ABCA1 (F) and ABCG1 (G) was determined.

(H) Young and old macrophage polarization. Expression of M1 (TNF- α , IL-6, IL1 β , PTGS2, CCL2, and MMP9) and M2 (IL-10, CD163, and TGF- β) markers was analyzed by qPCR.

Values are expressed as mean + SD (B) and mean + SE (C and E-H). Statistically significant difference, * p < 0.05, ** p < 0.01, *** p < 0.001.

expression signature is characteristic of proangiogenic macrophages (Apte et al., 2006; Mantovani et al., 2005; Mosser, 2003). In contrast, loss of *Abcg1* had no effect on global macrophage polarization to either classical or alternatively activated cells, as both IL-6 gene expression and IL-10 gene expression were reduced significantly (Figure S3A).

Next, we investigated the ability of *Abca1*^{-M/-M} and *Abcg1*^{-/-} macrophages to inhibit vascular endothelial cell proliferation in vitro using HMVECs and to regulate pathologic angiogenesis in vivo using the injury-induced CNV assay, as described previously and in the Experimental Procedures (Kelly et al., 2007). In cocultures, *Abca1*^{-M/-M} macrophages from young mice lost their ability to inhibit HMVECs proliferation as compared to macrophages from age-matched WT mice or from *Abcg1*^{-/-} young macrophages (Figure 3B and Figure S3B). These results, combined with previous findings that old macrophages lose the ability to regulate vascular proliferation and CNV, suggest that *Abca1*^{-M/-M} macrophages demonstrate an accelerated senescence program. We investigated this in vivo in the injury-induced CNV model. As anticipated, CNV volumes were significantly higher in mice whose macrophages were deficient in *Abca1* as compared to WT littermates (Figures 3C and 3D). In contrast, CNV volumes in *Abcg1*^{-/-} mice were comparable to littermate controls, confirming an ability of these cells to inhibit CNV (Figures S3C and S3D). We next explored whether loss of *Abca1* in macrophages altered the expression of VEGF, a well-documented angiogenic factor that promotes endothelial cell growth. Analysis of VEGF production by WT and *Abca1*^{-M/-M} macrophages by ELISA revealed that there was no significant difference (Figure S3E). Our findings suggest that the proangiogenic phenotype of ABCA1-deficient macrophage is VEGF independent. Taken together, these results demonstrate that ABCA1 is the primary regulator of macrophage polarization and that “young” macrophages lacking *Abca1* have the same cytokine polarization and functional deficits, i.e., proangiogenic behavior, as “old” WT macrophages.

Cholesterol-Rich Diet Accelerated a Senescent Macrophage Phenotype

As shown in Figure 2, ABCA1/G1 transporters within macrophages regulate intracellular cholesterol efflux. We next investigated the effect of chronic dietary lipid/cholesterol burden on macrophage function using diet-induced obesity (DIO) mice as a model of high-fat/cholesterol-fed mice. Quantitative analysis of intracellular cholesterol content demonstrated that DIO macrophages had significantly higher levels of total cholesterol compared to age-matched controls at both 3 and 6 months of age (Figure 3E). To determine whether high fat/cholesterol stress altered the ability of DIO macrophages to regulate vascular proliferation, we incubated young DIO macrophages with HMVECs and assessed their proliferation. DIO macrophages were unable to inhibit HMVECs proliferation (Figure 3F). In addition, DIO macrophages demonstrated an impaired ability to regulate CNV in vivo (Figures 3G and 3H), indicating that chronic fat/cholesterol stress can impair the ability of macrophages from young mice to regulate pathological vascular proliferation and angiogenesis. Quantification of plasma lipid and cholesterol levels showed an increase in 3-month-old DIO mice as compared to controls (FFA, 0.77 ± 0.044 versus 0.52 ± 0.008 mM; TG,

67.5 ± 12.9 versus 32.5 ± 3.9 mg/dl; cholesterol, 132.3 ± 13.6 versus 109.1 ± 2.8 mg/dl). These data also suggest that higher dietary lipid can potentially accelerate the programmatic changes associated with senescence within macrophages.

Enhancing Efflux in Senescent Macrophages Restored Their Functional Capacity to Regulate Pathological Angiogenesis

Our data show that age-associated reduction in expression of ABC transporters impairs the efflux capacity of macrophages and results in increased cholesterol accumulation. Loss of *Abca1* also translated into a loss of the ability of these cells to regulate angiogenesis. We therefore investigated whether restoring the efflux capacity of macrophages in old mice could improve their effector functions. Recent studies have shown that transcriptional nuclear receptors such as liver X receptors (LXRs) were direct enhancers of ABC transporter expression in macrophages (Repa et al., 2000).

Treatment of peritoneal young or old macrophages with LXR synthetic agonist (T0-901317) induced a dose-dependent upregulation of both ABCA1 and ABCG1 gene expression (Figures 4A and 4B). Treatment of old macrophages with LXR agonists allowed old cells to reach (at lower doses of agonist) and even exceed (at higher doses) the expression levels of ABCA1 seen in young macrophages. Increased expression of ABCG1 in old macrophages after treatment with LXR agonist was comparable to that seen in young macrophages.

Although the ability of old macrophages to upregulate ABCA1/G1 transporter expression in response to exogenous cholesterol (oxLDL) was dampened, as seen in Figures 2F and 2G, they were able to respond robustly to direct LXR stimulation by synthetic ligand (T0-901317). It has been previously demonstrated that LXR can be regulated by endogenously synthesized cholesterol oxidation products (oxysterols) such as 27-hydroxycholesterol (27-HC) or nonoxysterol mediators (T0-901317) (Janowski et al., 1996; Repa and Mangelsdorf, 1999; Repa et al., 2000). An analysis of cell-associated oxysterol content of young and old macrophages at baseline showed a 2-fold increase in 27-HC in old macrophages (Figure 4C). The increase in 27-HC was accompanied by a commensurate 2-fold increase in 7-ketocholesterol (7-KC). While 27-HC is an activator of the LXR pathway (Fu et al., 2001), numerous studies have shown that 7-KC can effectively interfere with LXR activation and cholesterol efflux (Gelissen et al., 1996, 1999; Kritharides et al., 1995). As seen in Figure 4C, the absolute increase in 7-KC levels was 17-fold greater than that of 27-HC, offering a possible explanation as to why old macrophages are unable to respond as efficiently to exogenous cholesterol stimulation but respond robustly to synthetic agonists.

These data suggest that it might be possible to reverse some of the programmatic dysfunctionality seen in these cells with age. In order to confirm this hypothesis, we cocultured LXR agonist (T0-901317)-treated young or old macrophages with HMVECs and analyzed their ability to inhibit endothelial cell proliferation. As shown in Figure 4D, LXR agonist treatment of old macrophages completely restored their ability to inhibit endothelial cell proliferation. Treatment of *Abca1*^{-M/-M} macrophages with LXR agonist does not restore their ability to inhibit HMVECs proliferation (Figures S4A and S4B). Interestingly, both young and

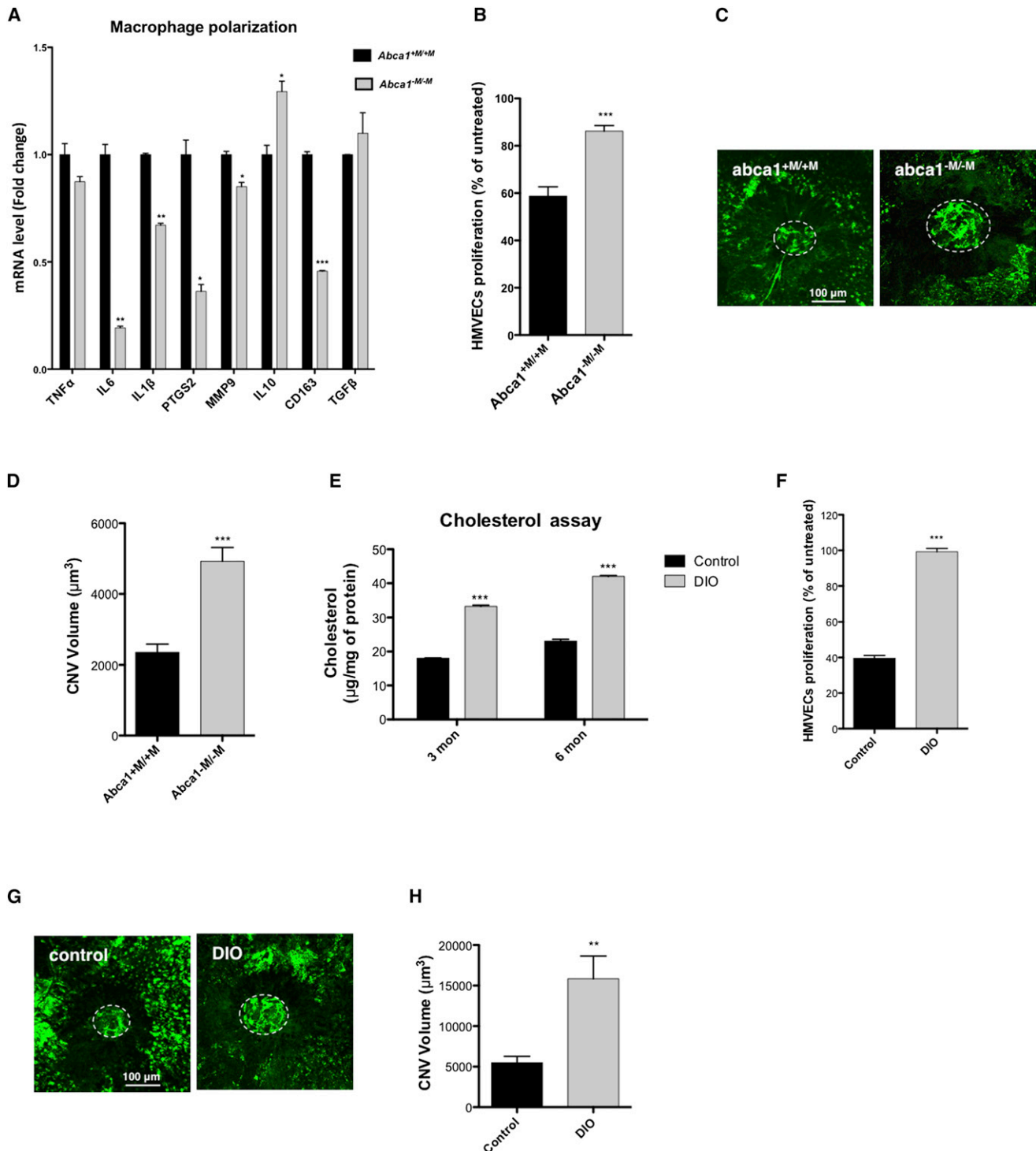


Figure 3. Macrophage Ability to Regulate Vascular Proliferation Is Altered by *Abca1* Deletion or Cholesterol-Rich Diet

(A) Quantitative mRNA analysis of M1 (TNF- α , IL-6, IL1 β , PTGS2, CCL2, and MMP9) and M2 (IL-10, CD163, and TGF- β) markers in WT (*Abca1*^{+/M/+M}) and *Abca1*-deficient (*Abca1*^{-M/-M}) peritoneal macrophages.

(B) HMVECs proliferation when cocultured with *Abca1*^{+/M/+M} or *Abca1*^{-M/-M} macrophages.

(C) *Abca1*^{+/M/+M} or *Abca1*^{-M/-M} mice were perfused with FITC-dextran (green) 7 days after laser injury, and CNV was examined by confocal microscopy. Representative CNV photographs are shown; scale bar, 100 μ m.

(D) Quantification of CNV (white circle) demonstrated a significant increase of CNV volume in *Abca1*^{-M/-M} mice compared to WT mice.

(E) Quantification of relative cholesterol content demonstrated a higher accumulation in macrophages from DIO mice at both 3 and 6 months of age as compared to controls.

(legend continued on next page)

old macrophages treated with LXR agonist (T0-901317 compound) exhibit features of classically activated M1 phenotype (Figure S4C).

These results confirm that downregulation of ABCA1 (not ABCG1) is the basis of the impaired function observed in old macrophages.

Old mice were then treated with intraperitoneal injections of vehicle (DMSO) or T0-901317 at 25 or 50 mg/kg/day for 5 days prior to laser induction of CNV. Quantitative analysis of gene expression showed that treated mice at both doses had strong systemic upregulation of ABCA1 and ABCG1 expression compared to vehicle-treated mice (Figures 4E–4G and Figures S4D and S4E). In addition, LXR-agonist treatment of old mice resulted in a significant and dose-dependent reduction in CNV compared to vehicle-treated old mice, thus restoring their functional capacity to regulate pathological vascular proliferation (Figures 4H and 4I). We further investigated whether local enhancement of macrophage efflux capacities can improve their regulation of CNV. Old mice were pretreated for 7 days with eye drops of vehicle or 4 mM of T0-901317 prior to induction of CNV. Quantitative analysis of ABCA1 and ABCG1 mRNA levels, after 7 additional days of eye drops treatment, showed a significant increase in the retina, brain, and liver (Figures S4F–S4I) of LXR agonist-treated mice as compared to vehicle-treated mice. Our findings also demonstrate that local LXR agonist treatment is as effective as systemic administration, given the fact that CNV volume is significantly reduced in old mice treated with eye drops of T0-901317 compared to vehicle (Figures S4J and S4K).

Taken together, these results conclusively demonstrate that direct induction of cholesterol efflux with synthetic LXR agonists locally or systemically restores in old macrophages effector capabilities that are similar to those observed in young macrophages.

Age-Related Reduction of ABCA1 Expression in Human PBMCs

The above data clearly demonstrate that senescent macrophages have impaired cholesterol efflux capacities that lead to a loss of their ability to regulate vascular proliferation. This impairment in macrophage function is associated with a loss of ABCA1. We next investigated the expression levels of ABCA1/G1 in PBMCs isolated from young (age range 25–34 years, $n = 9$) and old (age range 67–87 years, $n = 9$) donors. Total protein extracts were analyzed for ABCA1/G1 expression, and representative immunoblots are shown in Figure 5A. Densitometric analysis normalized to β -actin expression showed that ABCA1 expression level was significantly reduced in old compared to young donors, while ABCG1 protein expression was unchanged (Figures 5B and 5C). These findings are consistent with quantitative gene expression analysis demonstrating that ABCA1 gene expression was 2.5-fold lower in old donors while ABCG1 expression was not significantly different (Figures S5A and S5B). In addition, PBMCs from old donors had higher levels of IL-10, CD163, and IL8 expression compared to young

donors, confirming their phenotype as alternatively activated cells (Figure S5C).

Immunohistochemistry of a CNV membrane isolated from a patient during subretinal surgery confirmed the presence of CD68-positive macrophages that have reduced ABCA1 expression when compared to other cell types within the lesion (Figure 5D, arrows).

Age-Related Overexpression of miR-33 Repressed Macrophage Regulation of Vascular Proliferation

We have shown that aging altered macrophage expression of ABCA1 and ABCG1 that resulted in defective cholesterol efflux and subsequent impairment in their capacity to regulate pathological angiogenesis. We next investigated the mechanisms that led to the age-associated decline in the expression of ABC transporters. To determine whether epigenetic mechanisms were involved in this process, we analyzed the methylation pattern of *Abca1* and *Abcg1* promoters by bisulfate-modified CpG Sanger sequencing. There was no significant difference in the frequency or pattern of methylation of the promoter regions of these genes between young and old macrophages (Figure S6A). Recent studies have shown that a highly conserved microRNA, miR-33, regulates the expression of genes involved in cellular cholesterol metabolism, among them ABCA1 and ABCG1 (Marquart et al., 2010; Najafi-Shoushtari et al., 2010; Rayner et al., 2010, 2011). We next examined miR-33 expression in young and old macrophages. As shown in Figure 6A, miR-33 expression was significantly higher in old macrophages as compared to young, consistent with reduced expression of ABCA1 and ABCG1 observed in aged macrophages. Analysis of miR-33 and its host gene, *SREBP-2*, expression revealed that in both young and old macrophage, miR-33 and *SREBP-2* are coexpressed and coordinately regulated after LXR agonist treatment or cholesterol loading (Figures S6B–S6D). Based on these findings, we hypothesized that antagonism of miR-33 in macrophages might enhance their regulation of vascular proliferation. Macrophages were transfected with LNA miR-33 inhibitor (anti-miR-33) or negative control inhibitor (con anti-miR), and expression of ABC transporters was assessed. MicroRNA efficient transfection delivery was confirmed using fluorescent LNA anti-miR, as shown in Figure 6B. Inhibition of miR-33 in young and old macrophages resulted in a significant increase in mRNA and protein levels of ABCA1 (Figures 6C and 6D). In addition, antagonism of endogenous miR-33 not only promoted the polarization of macrophages to M1 phenotype (Figures S6E and S6F) but also improved the ability of young and old macrophages to inhibit vascular endothelial cell proliferation (Figure 6E). More importantly, improvement of the ability of macrophages to regulate vascular proliferation is ABCA1 dependent, as the inhibition of miR-33 in *Abca1*^{-M/-M} macrophages had no effect on their regulation of endothelial cell proliferation (Figure S6G). So far we have shown that macrophages from old mice exhibit impaired regulation of CNV in vivo and vascular endothelial cell proliferation in vitro. As these effects are

(F) Measurement of proliferation of HMVECs after incubation with DIO or control macrophages.

(G and H) Representative illustration (G) and quantification of CNV (white circle) volume (H) demonstrated an inability of DIO macrophages to inhibit CNV as compared to controls.

Values are expressed as mean + SE. Statistically significant difference, ** $p < 0.01$, *** $p < 0.001$.

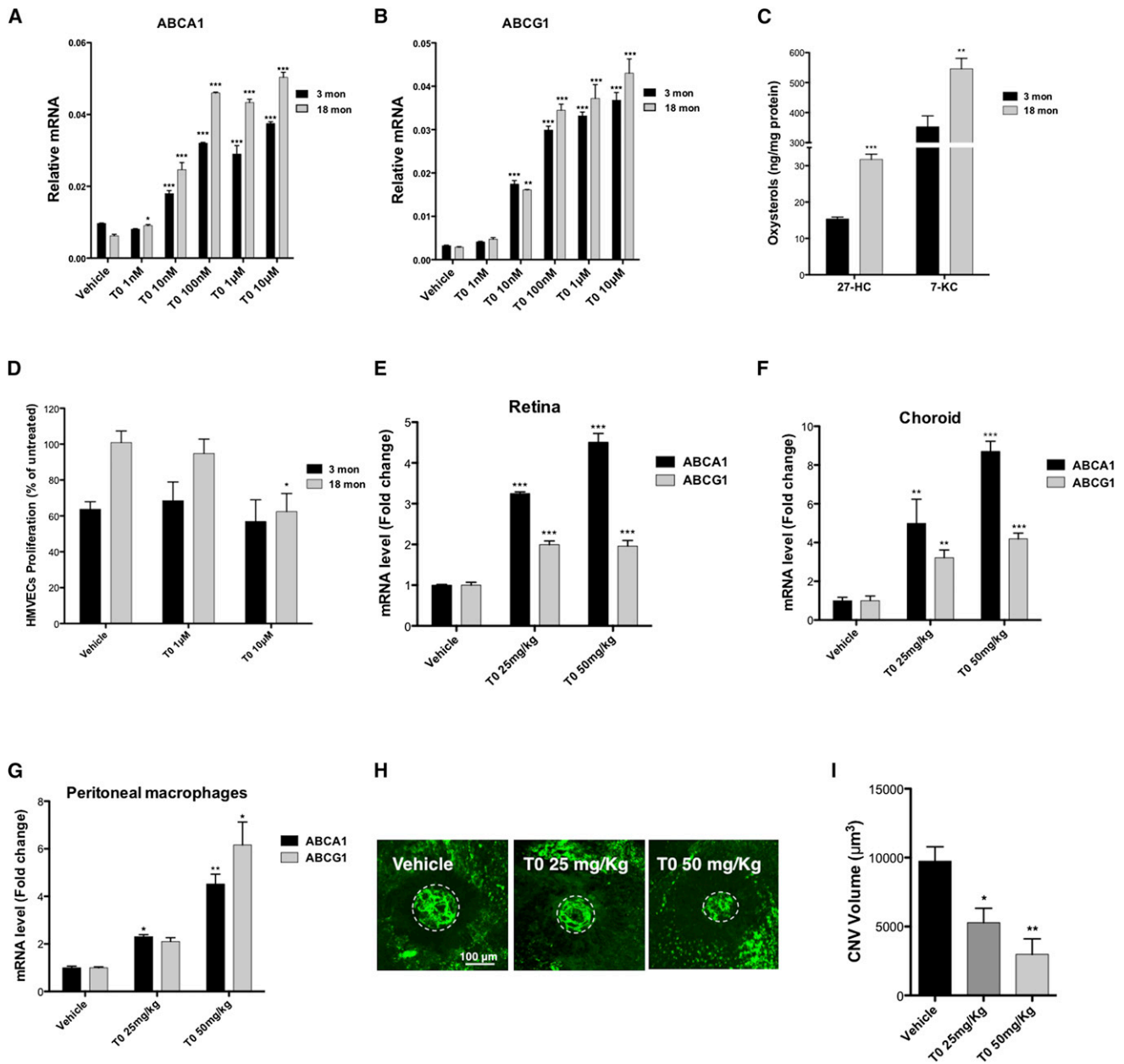


Figure 4. LXR Agonist Treatment Restored the Functional Capacities of Senescent Macrophages

(A and B) Peritoneal macrophages isolated from young and old mice were treated with vehicle, 1 nM to 10 μM of T0-901317 (T0), and quantitative analysis of ABCA1 (A) and ABCG1 (B) gene expression was performed by real-time qPCR.

(C) Oxysterols (27-hydroxycholesterol [27-HC] and 7-ketocholesterol [7-KC]) extracted from culture medium of young or old peritoneal macrophages were quantified by HPLC/MS and normalized to macrophage protein content.

(D) Effect of T0-901317 treatment on the ability of macrophages to inhibit HMVECs proliferation.

(E–G) Quantitative mRNA levels of ABCA1 and ABCG1 in retina (E), choroid (F), and peritoneal macrophages (G) of old mice, treated for 5 consecutive days with vehicle, 25 mg/kg, or 50 mg/kg of T0-901317.

(H and I) (H) Representative CNV images in vehicle and LXR agonist-treated old mice and quantification (I) of CNV (white circle) volume show a dose-dependent reduction of endothelial cell proliferation.

Values are expressed as mean + SE. Statistically significant difference, **p* < 0.05, ***p* < 0.01, ****p* < 0.001, compared to vehicle treatment.

associated with ABCA1 downregulation, we explored whether silencing of miR-33 could restore macrophage function and their ability to inhibit CNV. Old mice were pretreated daily with intra-peritoneal injection of 10 mg/kg LNA negative control anti-miR

or anti-miR-33 for 7 days prior to induction of CNV. After an additional 7 days of treatment, the quantitative mRNA analysis revealed that ABCA1 level was significantly higher in the choroid (Figure 6F) and retina (Figures S6H and S6I) of old mice treated

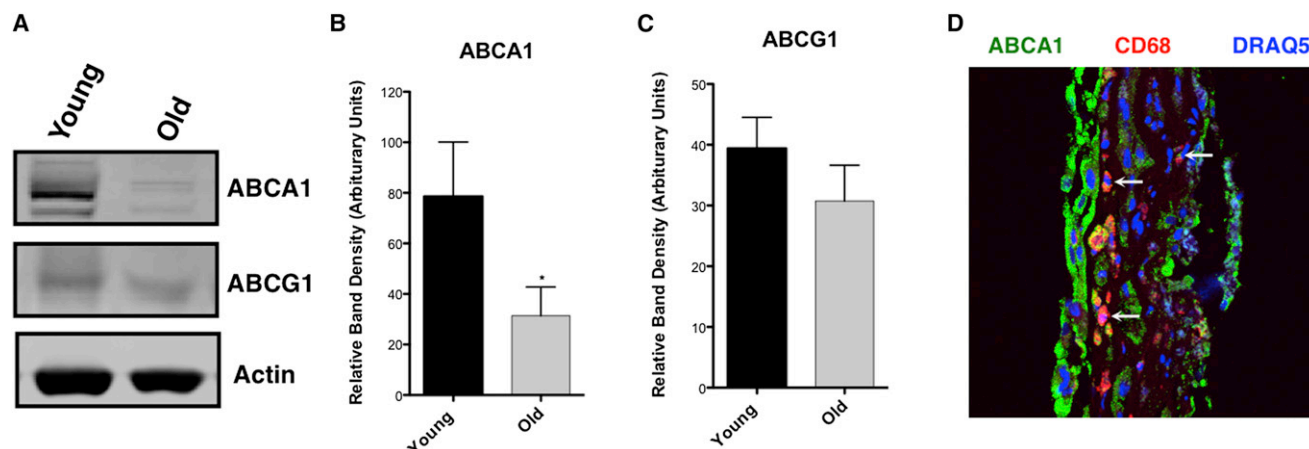


Figure 5. Age-Related Alteration of ABCA1 Expression in Human PBMCs

(A–C) (A) Western blot analysis of proteins extracted from PBMCs of young (<35 years old) or old (>65 years old) donors. Immunoblots were probed with antibodies against ABCA1, ABCG1, or β -actin. Relative quantification of ABCA1 (B) and ABCG1 (C) band densities.

(D) Immunohistochemistry of a CNV sample isolated from a patient after subretinal surgery with antibodies against ABCA1 (green) or CD68 (macrophage marker, red). Nuclei were stained with Draq5 (blue). Values are expressed as mean \pm SE. Statistically significant difference, * $p < 0.05$.

with anti-miR-33 compared to control-treated mice. In addition, inhibition of miR-33 also induced a significant increase of ABCA1 protein levels (Figure 6G). As shown in Figures 6H and 6I, antagonism of miR-33 in old mice resulted in significantly decreased CNV compared to control-treated old mice.

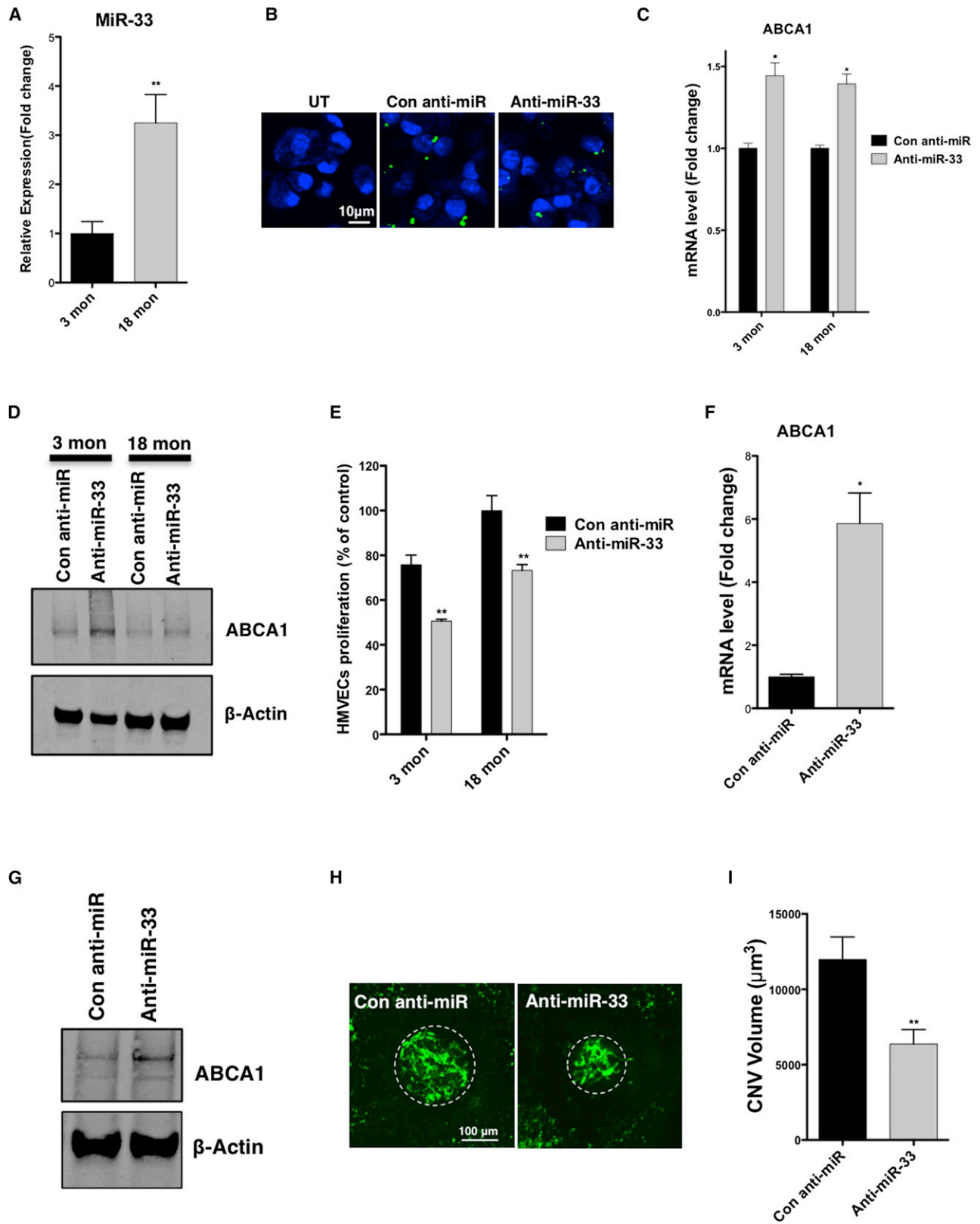
DISCUSSION

Clear parallels exist between atherosclerosis and AMD. Atherosclerosis is characterized by subvascular endothelial ApoB-LP focal deposition in the form of plaques (Moore and Tabas, 2011). AMD is characterized by the development of subretinal drusen, which are highly enriched for esterified-cholesterol rich ApoB-LP (Curcio et al., 2010). Macrophage-mediated plaque progression and inflammation can eventually lead to plaque necrosis, rupture, and death. In AMD, chronic age-associated changes program macrophages to a disease-promoting proangiogenic phenotype that renders these cells unable to regulate the growth of abnormal blood vessels within the central retina called the macula (Kelly et al., 2007; Klein et al., 2004). These aberrant vessels are responsible for bleeding that can lead to severe vision loss and blindness. Although macrophages have been shown to interact with and process lipid-rich material in drusen, the precise molecular mechanisms that cause senescent macrophages to promote progression from drusen to neovascularization in the eye were previously unknown.

In these studies, we have demonstrated that the cholesterol efflux regulators ABCA1 and ABCG1 are downregulated in macrophages with age in both mice and humans. Age-associated downregulation of ABCA1 leads to alternative proangiogenic polarization of macrophages to an M2-like disease-promoting phenotype. This is especially interesting in the light of previous studies that have shown that older mice have significantly higher volumes of CNV (Kelly et al., 2007) after injury and that advanced AMD (van Leeuwen et al., 2003) characterized by CNV only develops in individuals over 50 years of age. Using loss-of-function

experiments with conditional knockout mice, we have been able to demonstrate that macrophages deficient in ABCA1 are unable to regulate CNV in vivo and vascular endothelial cell proliferation in vitro. In essence, *Abca1*^{-M/-M} macrophages functionally behave like senescent macrophages isolated from mice at least 18 months of age. Of interest, loss of *Abcg1* does not seem to affect the ability of these cells to regulate CNV or vascular endothelial proliferation, suggesting a dominant role for ABCA1 in this process. In addition, our results also suggest that these effects are VEGF independent. A potential reason for the ABCA1 dominance in this process is the complete polarization of *Abca1*^{-M/-M} macrophages to an M2 phenotype identical to that seen in senescent macrophages that are unable to regulate aberrant angiogenesis. By contrast, *Abcg1*^{-/-} macrophages have a mixed phenotype, which may explain why they retain their functional abilities and do not demonstrate a programmatic shift to a senescent phenotype. It is also possible that ABCA1-driven efflux of intracellular cholesterol to the cell surface prior to deposition on to lipid-poor ApoA-1 is the critical pathway involved in the ability of macrophages to regulate aberrant and proliferative angiogenesis.

Experiments in DIO mice have also provided insights into the effects of cholesterol loading on macrophage function in the eye. Macrophages from mice fed a high-fat diet for a period of up to 6 months are unable to regulate CNV in vivo and vascular endothelial cell proliferation in vitro. These findings shed light on conflicting data from genetic and epidemiologic studies that demonstrate a complex association between polymorphisms in genes that regulate HDL and cholesterol metabolism and AMD as outlined above (Chen et al., 2010; Neale et al., 2010). The data from knockout mice and the reduced expression of ABC transporters from old humans, diagnosed with AMD, suggest that local regulation of cholesterol efflux in the eye and the ability of macrophages to efficiently transport cholesterol from drusen to HDL and onto the systemic circulation are critical for the prevention of triggering of drusen-induced CNV in AMD.



(legend on next page)

In older animals and humans, macrophages lose their ability to efflux cholesterol efficiently. This leads to alternative proangiogenic polarization of these cells, which in the appropriate genetic context of polymorphisms in complement regulatory genes (Edwards et al., 2005), and alongside environmental cues such as smoking, can create a lethal microenvironment for the development and progression of advanced AMD where new blood vessels proliferate, cause bleeding, and induce the formation of scar tissue that leads to photoreceptor loss and blindness. Cholesterol-loading experiments with DIO mice suggest that this process may be modified and accelerated by dietary lipid.

Our gain-of-function studies demonstrate that by upregulating ABC transporter expression in senescent macrophages using LXR agonists, we are able to restore their ability to inhibit vascular endothelial cell proliferation and CNV. In essence, LXR agonists are able to reverse the senescent phenotype and restore their angioregulatory function to levels comparable to mice that are significantly younger. Our work also revealed that upregulation of miR-33 in aged macrophages might be responsible for the repression of ABCA1 that leads to defective cellular cholesterol metabolism in senescent macrophages. We have shown that despite increased cholesterol accumulation in old macrophages, SREBP-2/miR-33 levels were higher when compared to young macrophages. Such cholesterol accumulation translated into a significant increase of production of diverse oxysterols with potentially different effects on cholesterol efflux and transport. Indeed, antagonism of endogenous miR-33 improves macrophage regulation of vascular proliferation and silencing of miR-33 in old mice, and results in specific and robust inhibition of CNV. Anti-miR-33 treatment polarizes macrophages to a classically activated phenotype that is reflected in the cytokine gene expression signature. These results have significant therapeutic implications. CNV in AMD accounts for a large majority of blindness from this disease. Therapeutic intervention prior to the development of advanced disease with effective agents that upregulate macrophage cholesterol efflux in the eye might prevent progression and can be used as prophylaxis against the development of CNV and its blinding complications. The ability to deliver such therapies locally to the eye is a unique advantage in this immune-privileged organ (Niederkorn, 2006) and may be an effective barrier to off-target complications that are often seen with systemic therapy.

EXPERIMENTAL PROCEDURES

Animals

All animal experiments were conducted in accordance with Washington University School of Medicine in St. Louis Animal Care and Use guidelines and af-

ter approval by the Animal Studies Committee. C57BL/6 mice (aged <6 months), diet-induced obese (DIO) mice, and age-matched controls were purchased from The Jackson Laboratory. C57BL/6 old mice (aged >18 months) were purchased from National Institute of Aging. Macrophage-specific *Abca1* knockout mice (*Abca1*^{-M/-M}) were generated by breeding *Abca1*^{flax/flax} mice, provided by Dr. John S Parks (Timmins et al., 2005), with Lys-M Cre mice (The Jackson Laboratory). Previously characterized *Abcg1*^{-/-} knockout mice (Baldán et al., 2006; Kennedy et al., 2005) were provided by Dr. Angel Baldán.

Cells

Splenic macrophages were isolated by positive selection as previously described (Apte et al., 2006). In brief, F4/80⁺ macrophages were purified from dissociated mouse spleen using magnetic separation (StemCell Technologies, Inc.). Peritoneal macrophage recruitment was elicited by intraperitoneal injection of 4% thioglycollate. Five days after injection, macrophages were harvested and cultured in RPMI-1640 overnight (GIBCO). Young or old mouse peripheral blood mononuclear cells (PBMCs) were prepared by centrifugation over Histopaque 1083 (Sigma-Aldrich) according to the manufacturer's instructions. Single-eye macrophages were isolated from CNV complexes (Figure S1C) by laser capture microdissection (LMD6000, Leica). Human dermal microvascular endothelial cells (HMVECs) were purchased from Lonza and cultured in EGM2V media. Human peripheral blood mononuclear cells were isolated from young (age range 25–34 years, n = 9) or old (age range 67–87 years, n = 9) donors diagnosed with neovascular AMD. This study was approved by the Human Research Protection Office of Washington University School of Medicine in St. Louis School, and informed consent was obtained from all blood donors. PBMCs were purified by density gradient centrifugation using BD Vacutainer CPT.

Real-Time PCR and Gene Expression Analysis

Total RNA was prepared from splenic macrophage, peritoneal macrophages, retina, choroid, or PBMCs using the RNeasy Mini Kit (QIAGEN). cDNA was prepared using the High Capacity cDNA Archive Kit (Applied Biosystems), and PCR amplifications of cDNA were performed using Taqman probe-based gene expression assay (Applied Biosystems) as previously described (Kelly et al., 2007).

Cholesterol Measurement

Total cholesterol content of young and old peritoneal macrophages was quantified using the Amplex Red Cholesterol Assay Kit (Molecular Probes). In brief, 50 μ l of cell lysates (diluted in reaction buffer supplied in the assay kit) were incubated with 50 μ l of the Amplex Red reagent/HRP/cholesterol oxidase/cholesterol esterase solution for 30 min at 37°C. At different time points, cholesterol-associated fluorescence was measured, and total cholesterol content was quantified using a cholesterol standard curve.

OxLDL Uptake Assay

Peritoneal macrophages isolated from young (<3 months) and old (\geq 18 months) mice were plated on chamber slides, and adherent cells were treated with 25 μ g/ml Dil-oxylized LDL (oxLDL) for 24 hr (Intracel). After multiple washes, Dil-oxLDL retention was examined using Zeiss LSM510 confocal microscope.

Figure 6. miR-33 Modulates Macrophage Regulation of Vascular Proliferation

- (A) Quantitative analysis of miR-33 in young and old peritoneal macrophages.
 (B) Representative photograph of macrophages untransfected (UT) or transfected with fluorescent LNA anti-miR. Macrophages isolated from 3- or 18-month-old mice were transfected with negative control anti-miR or anti-miR-33.
 (C and D) Twenty-four hours after transfection, mRNA (C) and protein (D) expression of ABCA1 were determined.
 (E) Effects of miR-33 antagonism on macrophage inhibition of HMVECs proliferation.
 (F and G) Old mice were pretreated daily with 10 mg/kg in vivo LNA, negative control anti-miR, or anti-miR-33 for 7 days prior to induction of CNV. (F) Mice were then treated for 7 additional days, and quantitative mRNA (F) and protein (G) level of ABCA1 in the choroid were analyzed.
 (H and I) Representative illustration (H) and CNV volume quantification (I) showed that in vivo antagonism of miR-33 induced an inhibition of vascular endothelial cell proliferation.

Values are expressed as mean + SE. Statistically significant difference, *p < 0.05, **p < 0.01.

Cholesterol Efflux Assay

Thioglycollate-elicited peritoneal macrophage from young (<3 months) and old (≥ 18 months) mice were incubated with 5 $\mu\text{Ci/ml}$ [^3H]cholesterol-labeled oxLDL for 24 hr. Cells were then washed and equilibrated with 2 mg/ml BSA (Sigma-Aldrich) in media for 1 hr followed by incubation for 4 hr in media containing 10 $\mu\text{g/ml}$ human ApoA1 or 50 $\mu\text{g/ml}$ human HDL. Supernatants were collected, and specific ApoA1/HDL-cholesterol efflux was expressed as a percentage relative to total radioactivity in cells and media.

Serum Analyses

Serum levels of lipids and cholesterol were determined as previously described (Chakravarthy et al., 2005). Mice were anesthetized, and blood was collected from the retro-orbital venous plexus with a capillary tube. Serum concentrations of free fatty acids (FFAs), triglycerides (TGs), and cholesterol were determined enzymatically using kits purchased from Sigma-Aldrich.

Vascular Endothelial Cell Proliferation Assay

Cell proliferation was measured with an adaptation of a previously described method (Khan and Apte, 2008). HMVECs (1×10^4 cells) in log phase were cultured in 96-well round-bottomed plates for adherence. HMVECs cells were then cocultured with peritoneal macrophages (1:25 ratio) and incubated with 5 $\mu\text{Ci/ml}$ [^3H] thymidine (PerkinElmer) for 24 hr. Cells were harvested onto glass fiber filters (Packard), and incorporated [^3H] thymidine was read using TopCount NXT (PerkinElmer).

Laser-Induced CNV in Mice

Rupture of Bruchs membrane with laser was used to initiate CNV in mice as described previously (Apte et al., 2006). Although this is an injury model of AMD, it has been highly predictive of the pathophysiology of and molecular mechanisms underlying neovascular AMD. Briefly, mice were anesthetized, and their pupils were dilated with 1% tropicamide. Using argon green laser, four laser burns were placed around the optic nerve (0.1 s, 50 μm , and 110 mW). Seven days after laser, mice were anesthetized and perfused intraventricularly with FITC-dextran (Sigma-Aldrich). Mice were euthanized in a CO_2 chamber, and their eyes were harvested for tissue processing. The choroidal flat mounts were analyzed for the presence of CNV by confocal microscopy. The extent of CNV was quantified by Metamorph Imaging software. We used $n \geq 5$ mice for each group.

LXR Agonist Treatment

Young and old peritoneal macrophages were treated with LXR agonist, T0-901317 (Sigma-Aldrich), for 24 hr. LXR agonist was dissolved in DMSO (vehicle), and treatment dosage ranged from 0 to 10 μM . Old mice (>18 months) were given a daily intraperitoneal injection of vehicle, 25 mg/kg or 50 mg/kg T0-901317. After 5 consecutive days of treatment, CNV was induced and analyzed as described above. Old mice were pretreated for 7 consecutive days with eye drops of vehicle or 4 mM T0-901317 prior to induction of CNV. After 7 additional days of eye drops treatment, CNV volume was quantified, and mRNA levels of ABCA1 and ABCG1 were analyzed in mouse tissues.

Oxysterol Determinations

Oxysterols were extracted from RPMI-1640 culture media of young or old peritoneal macrophages, and determinations of 27-hydroxycholesterol (27-HC) and 7-ketocholesterol (7-KC) were performed as previously described (Jiang et al., 2011).

MicroRNA Quantification

Total miRNA was isolated from peritoneal macrophages using mirVana kit (Ambion) and reverse transcribed with the RT² miRNA First Strand Kit (SABioscience). PCR amplifications of cDNA were performed using RT² SYBR Green qPCR (SABioscience) with specific primers for quantification of mouse miR-33 and normalized to U6 as housekeeping gene.

Antagonism of miR-33

Peritoneal macrophages were transfected with 50 nM LNA (locked nucleic acid) miR-33 inhibitor (anti-miR-33) or negative control inhibitor (con anti-miR) (Exiqon) using HiPerFect Transfection reagent (QIAGEN). The transfection efficiency of macrophages was assessed using fluorescent LNA anti-miR (Exiqon). After miR-33 inhibition, target genes and proteins were analyzed by qPCR and western blotting.

Old mice were pretreated for 7 days with daily intraperitoneal injection of 10 mg/kg in vivo LNA anti-miR-33 or control anti-miR (Exiqon), prior to induction of CNV. After 7 additional days of treatment, CNV volume was quantified, and the expression of miR-33 targets was analyzed in mouse tissues by qPCR and western blotting.

Old mice were pretreated for 7 days with daily intraperitoneal injection of 10 mg/kg in vivo LNA anti-miR-33 or control anti-miR (Exiqon), prior to induction of CNV. After 7 additional days of treatment, CNV volume was quantified, and the expression of miR-33 targets was analyzed in mouse tissues by qPCR and western blotting.

Statistics

Statistical analysis was determined by two-tailed Student's t test and ANOVA with the use of GraphPad Prism Software. The error bars represent standard SEM, except in Figure 2B, where errors bars represent SD. Statistical significance was defined at $p < 0.05$.

SUPPLEMENTAL INFORMATION

Supplemental Information includes six figures and Supplemental Experimental Procedures and can be found with this article at <http://dx.doi.org/10.1016/j.cmet.2013.03.009>.

ACKNOWLEDGMENTS

This work was supported by NIH grant K08EY016139 (R.S.A.); NIH grant R01EY019287 (R.S.A.); NIH Vision Core Grant P30EY02687, U.S. Civilian Research and Development Foundation (R.S.A. and I.C.); NIH grants P01HL049373 (J.S.P.) and R01 HL094525 (J.S.P.); NIH grant R01 HL067773 (D.S.O.); NIH grant HL-107794 (A.B.); NIH grant HL-30568 (P.A.E.); the Carl Marshall Reeves and Mildred Almen Reeves Foundation Inc. Award (R.S.A.); the Research to Prevent Blindness Inc. Career Development Award (R.S.A.); the International Retina Research Foundation (R.S.A.); the American Health Assistance Foundation (R.S.A.); the Lacy Foundation Research Award (A.S.); the Thome Foundation (R.S.A.); and a Research to Prevent Blindness Inc. Unrestricted Grant to Washington University. Mass spectrometry and mouse serum analysis, respectively, were performed in the Metabolomics Facility and the Diabetes Research Center (NIH P60 DK 20579) at Washington University in Saint Louis. The authors would like to acknowledge the insights and constructive input of Drs. Douglas Green, Jayakrishna Ambati, Steve Teitelbaum, Shiming Chen, and Thomas Ferguson regarding these studies. R.S.A. is named as an inventor in a patent application filed by Washington University on the intellectual property presented in this article.

Received: April 29, 2012

Revised: January 21, 2013

Accepted: March 18, 2013

Published: April 2, 2013

REFERENCES

- Apte, R.S., Richter, J., Herndon, J., and Ferguson, T.A. (2006). Macrophages inhibit neovascularization in a murine model of age-related macular degeneration. *PLoS Med.* 3, e310. <http://dx.doi.org/10.1371/journal.pmed.0030310>.
- Baldán, A., Tarr, P., Vales, C.S., Frank, J., Shimotake, T.K., Hawgood, S., and Edwards, P.A. (2006). Deletion of the transmembrane transporter ABCG1 results in progressive pulmonary lipidosis. *J. Biol. Chem.* 281, 29401–29410.
- Bressler, S.B., Maguire, M.G., Bressler, N.M., and Fine, S.L.; The Macular Photocoagulation Study Group. (1990). Relationship of drusen and abnormalities of the retinal pigment epithelium to the prognosis of neovascular macular degeneration. *Arch. Ophthalmol.* 108, 1442–1447.
- Chakravarthy, M.V., Pan, Z., Zhu, Y., Tordjman, K., Schneider, J.G., Coleman, T., Turk, J., and Semenkovich, C.F. (2005). "New" hepatic fat activates PPARalpha to maintain glucose, lipid, and cholesterol homeostasis. *Cell Metab.* 1, 309–322.
- Chen, W., Stambolian, D., Edwards, A.O., Branham, K.E., Othman, M., Jakobsdottir, J., Tosakulwong, N., Pericak-Vance, M.A., Campochiaro, P.A., Klein, M.L., et al.; Complications of Age-Related Macular Degeneration Prevention Trial Research Group. (2010). Genetic variants near TIMP3 and

- high-density lipoprotein-associated loci influence susceptibility to age-related macular degeneration. *Proc. Natl. Acad. Sci. USA* 107, 7401–7406.
- Curcio, C.A., Millican, C.L., Bailey, T., and Kruth, H.S. (2001). Accumulation of cholesterol with age in human Bruch's membrane. *Invest. Ophthalmol. Vis. Sci.* 42, 265–274.
- Curcio, C.A., Presley, J.B., Malek, G., Medeiros, N.E., Avery, D.V., and Kruth, H.S. (2005). Esterified and unesterified cholesterol in drusen and basal deposits of eyes with age-related maculopathy. *Exp. Eye Res.* 81, 731–741.
- Curcio, C.A., Johnson, M., Huang, J.D., and Rudolf, M. (2009). Aging, age-related macular degeneration, and the response-to-retention of apolipoprotein B-containing lipoproteins. *Prog. Retin. Eye Res.* 28, 393–422.
- Curcio, C.A., Johnson, M., Huang, J.D., and Rudolf, M. (2010). Apolipoprotein B-containing lipoproteins in retinal aging and age-related macular degeneration. *J. Lipid Res.* 51, 451–467.
- Edwards, A.O., Ritter, R., 3rd, Abel, K.J., Manning, A., Panhuysen, C., and Farrer, L.A. (2005). Complement factor H polymorphism and age-related macular degeneration. *Science* 308, 421–424.
- Fu, X., Menke, J.G., Chen, Y., Zhou, G., MacNaul, K.L., Wright, S.D., Sparrow, C.P., and Lund, E.G. (2001). 27-hydroxycholesterol is an endogenous ligand for liver X receptor in cholesterol-loaded cells. *J. Biol. Chem.* 276, 38378–38387.
- Gelissen, I.C., Brown, A.J., Mander, E.L., Kritharides, L., Dean, R.T., and Jessup, W. (1996). Sterol efflux is impaired from macrophage foam cells selectively enriched with 7-ketocholesterol. *J. Biol. Chem.* 271, 17852–17860.
- Gelissen, I.C., Rye, K.A., Brown, A.J., Dean, R.T., and Jessup, W. (1999). Oxysterol efflux from macrophage foam cells: the essential role of acceptor phospholipid. *J. Lipid Res.* 40, 1636–1646.
- Hageman, G.S., Luthert, P.J., Victor Chong, N.H., Johnson, L.V., Anderson, D.H., and Mullins, R.F. (2001). An integrated hypothesis that considers drusen as biomarkers of immune-mediated processes at the RPE-Bruch's membrane interface in aging and age-related macular degeneration. *Prog. Retin. Eye Res.* 20, 705–732.
- Janowski, B.A., Willy, P.J., Devi, T.R., Falck, J.R., and Mangelsdorf, D.J. (1996). An oxysterol signalling pathway mediated by the nuclear receptor LXR alpha. *Nature* 383, 728–731.
- Jiang, X., Sidhu, R., Porter, F.D., Yanjanin, N.M., Speak, A.O., te Vrugte, D.T., Platt, F.M., Fujiwara, H., Scherrer, D.E., Zhang, J., et al. (2011). A sensitive and specific LC-MS/MS method for rapid diagnosis of Niemann-Pick C1 disease from human plasma. *J. Lipid Res.* 52, 1435–1445.
- Kelly, J., Ali Khan, A., Yin, J., Ferguson, T.A., and Apte, R.S. (2007). Senescence regulates macrophage activation and angiogenic fate at sites of tissue injury in mice. *J. Clin. Invest.* 117, 3421–3426.
- Kennedy, M.A., Barrera, G.C., Nakamura, K., Baldán, A., Tarr, P., Fishbein, M.C., Frank, J., Francone, O.L., and Edwards, P.A. (2005). ABCG1 has a critical role in mediating cholesterol efflux to HDL and preventing cellular lipid accumulation. *Cell Metab.* 1, 121–131.
- Khan, A.A., and Apte, R.S. (2008). An assay for macrophage-mediated regulation of endothelial cell proliferation. *Immunobiology* 213, 695–699.
- Klein, R., Peto, T., Bird, A., and Vannewkirk, M.R. (2004). The epidemiology of age-related macular degeneration. *Am. J. Ophthalmol.* 137, 486–495.
- Kritharides, L., Jessup, W., Mander, E.L., and Dean, R.T. (1995). Apolipoprotein A-I-mediated efflux of sterols from oxidized LDL-loaded macrophages. *Arterioscler. Thromb. Vasc. Biol.* 15, 276–289.
- Mantovani, A., Sica, A., Sozzani, S., Allavena, P., Vecchi, A., and Locati, M. (2004). The chemokine system in diverse forms of macrophage activation and polarization. *Trends Immunol.* 25, 677–686.
- Mantovani, A., Sica, A., and Locati, M. (2005). Macrophage polarization comes of age. *Immunity* 23, 344–346.
- Marquart, T.J., Allen, R.M., Ory, D.S., and Baldán, A. (2010). miR-33 links SREBP-2 induction to repression of sterol transporters. *Proc. Natl. Acad. Sci. USA* 107, 12228–12232.
- Moore, K.J., and Tabas, I. (2011). Macrophages in the pathogenesis of atherosclerosis. *Cell* 145, 341–355.
- Mosser, D.M. (2003). The many faces of macrophage activation. *J. Leukoc. Biol.* 73, 209–212.
- Najafi-Shoushtari, S.H., Kristo, F., Li, Y., Shioda, T., Cohen, D.E., Gerszten, R.E., and Näär, A.M. (2010). MicroRNA-33 and the SREBP host genes cooperate to control cholesterol homeostasis. *Science* 328, 1566–1569.
- Nakamura, K., Kennedy, M.A., Baldán, A., Bojanic, D.D., Lyons, K., and Edwards, P.A. (2004). Expression and regulation of multiple murine ATP-binding cassette transporter G1 mRNAs/isoforms that stimulate cellular cholesterol efflux to high density lipoprotein. *J. Biol. Chem.* 279, 45980–45989.
- Nakao, S., Kuwano, T., Tsutsumi-Miyahara, C., Ueda, S., Kimura, Y.N., Hamano, S., Sonoda, K.H., Saijo, Y., Nukiwa, T., Strieter, R.M., et al. (2005). Infiltration of COX-2-expressing macrophages is a prerequisite for IL-1 beta-induced neovascularization and tumor growth. *J. Clin. Invest.* 115, 2979–2991.
- Neale, B.M., Fagermess, J., Reynolds, R., Sobrin, L., Parker, M., Raychaudhuri, S., Tan, P.L., Oh, E.C., Merriam, J.E., Souied, E., et al. (2010). Genome-wide association study of advanced age-related macular degeneration identifies a role of the hepatic lipase gene (LIPC). *Proc. Natl. Acad. Sci. USA* 107, 7395–7400.
- Niederhorn, J.Y. (2006). See no evil, hear no evil, do no evil: the lessons of immune privilege. *Nat. Immunol.* 7, 354–359.
- Rayner, K.J., Suárez, Y., Dávalos, A., Parathath, S., Fitzgerald, M.L., Tamehiro, N., Fisher, E.A., Moore, K.J., and Fernández-Hernando, C. (2010). miR-33 contributes to the regulation of cholesterol homeostasis. *Science* 328, 1570–1573.
- Rayner, K.J., Sheedy, F.J., Esau, C.C., Hussain, F.N., Temel, R.E., Parathath, S., van Gils, J.M., Rayner, A.J., Chang, A.N., Suarez, Y., et al. (2011). Antagonism of miR-33 in mice promotes reverse cholesterol transport and regression of atherosclerosis. *J. Clin. Invest.* 121, 2921–2931.
- Repa, J.J., and Mangelsdorf, D.J. (1999). Nuclear receptor regulation of cholesterol and bile acid metabolism. *Curr. Opin. Biotechnol.* 10, 557–563.
- Repa, J.J., Turley, S.D., Lobaccaro, J.A., Medina, J., Li, L., Lustig, K., Shan, B., Heyman, R.A., Dietschy, J.M., and Mangelsdorf, D.J. (2000). Regulation of absorption and ABC1-mediated efflux of cholesterol by RXR heterodimers. *Science* 289, 1524–1529.
- Tall, A.R., Yvan-Charvet, L., Terasaka, N., Pagler, T., and Wang, N. (2008). HDL, ABC transporters, and cholesterol efflux: implications for the treatment of atherosclerosis. *Cell Metab.* 7, 365–375.
- Tarling, E.J., and Edwards, P.A. (2011a). ATP binding cassette transporter G1 (ABCG1) is an intracellular sterol transporter. *Proc. Natl. Acad. Sci. USA* 108, 19719–19724.
- Tarling, E.J., and Edwards, P.A. (2011b). Dancing with the sterols: critical roles for ABCG1, ABCA1, miRNAs, and nuclear and cell surface receptors in controlling cellular sterol homeostasis. *Biochim. Biophys. Acta.* 1821, 386–395.
- Timmins, J.M., Lee, J.Y., Boudyguina, E., Kluckman, K.D., Brunham, L.R., Mulya, A., Gebre, A.K., Coutinho, J.M., Colvin, P.L., Smith, T.L., et al. (2005). Targeted inactivation of hepatic Abca1 causes profound hypoalphalipoproteinemia and kidney hypercatabolism of apoA-I. *J. Clin. Invest.* 115, 1333–1342.
- van Leeuwen, R., Klaver, C.C., Vingerling, J.R., Hofman, A., and de Jong, P.T. (2003). Epidemiology of age-related maculopathy: a review. *Eur. J. Epidemiol.* 18, 845–854.
- Vedhachalam, C., Duong, P.T., Nickel, M., Nguyen, D., Dhanasekaran, P., Saito, H., Rothblat, G.H., Lund-Katz, S., and Phillips, M.C. (2007). Mechanism of ATP-binding cassette transporter A1-mediated cellular lipid efflux to apolipoprotein A-I and formation of high density lipoprotein particles. *J. Biol. Chem.* 282, 25123–25130.
- Wang, L., Clark, M.E., Crossman, D.K., Kojima, K., Messinger, J.D., Mobley, J.A., and Curcio, C.A. (2010). Abundant lipid and protein components of drusen. *PLoS ONE* 5, e10329. <http://dx.doi.org/10.1371/journal.pone.0010329>.
- Zhu, X., Lee, J.Y., Timmins, J.M., Brown, J.M., Boudyguina, E., Mulya, A., Gebre, A.K., Willingham, M.C., Hiltbold, E.M., Mishra, N., et al. (2008). Increased cellular free cholesterol in macrophage-specific Abca1 knock-out mice enhances pro-inflammatory response of macrophages. *J. Biol. Chem.* 283, 22930–22941.